

# STUDY OF AN ORGANIC RANKINE CYCLE ASSOCIATED TO A BIOMASS-FUELLED BOILER FOR COGENERATION APPLICATION

Sylvain QUOILIN, Vincent LEMORT, Jean LEBRUN  
Laboratoire de thermodynamique - Université de Liège  
Campus du Sart-Tilman, B-49  
B-4000 Liège, Belgium  
[squoilin@ulg.ac.be](mailto:squoilin@ulg.ac.be)

## ABSTRACT

This paper presents a cogeneration system composed of a biomass-fuelled boiler and of an Organic Rankine Cycle (ORC). The first part of the paper describes the model of the system. This model is built by interconnecting the sub-models of the different components: heat exchangers, pump, boiler and scroll expander.

In the second part, the results of an experimental study are presented : this study aimed at evaluating the performances of an ORC working with refrigerant R-123 and using scroll expander. The above models are validated using test results.

The last part of the paper investigates, through simulations, the performances of the cogeneration system and points out some possible improvements.

## INTRODUCTION

Micro and mini cogeneration applications require power cycles to produce electricity. The internal combustion engine shows good performances, but only tolerates very specific fuels. In the case of biomass combustion, an external combustion engine is more appropriate.

The two common solutions for external combustion engine are the Stirling engine and the organic Rankine cycle (ORC). ORC's present the advantage of being very easy to set up and use widely available components.

The approach selected in this work is to study a cogeneration module that could work with minimal modifications on the boiler: the heat is transported from the boiler to the evaporator of the cycle by means of a primary circuit, without modifying the boiler design. Heat for space heating is then recovered at the condenser of the cycle. Heat source temperature is lower than in traditional cogeneration plants and the efficiency of the cycle is thus slightly sacrificed at the profit of simplicity and lower investment cost.

The choice of the ORC working fluid is a key issue, since it affects the efficiency and the size of the plant. Past studies have shown the influence of working fluid thermodynamic properties on the ORC performances (Hung, 2001; Liu et al., 2004; Maizza et al., 2001). Several fluids will be simulated in this work in order to select the best candidate.

Another key issue is the choice of the expander. Platell (1993) showed that positive displacement expanders are more adapted than turbo-expanders to small scale units. Scroll expanders have been studied in a number of papers (Zanelli, 1994, Kane, 2002; Manzagol et al., 2002; Xiaojun et al., 2004; Yuanyang et al., 2006; Lemort et al, 2006), and show very promising performances.

This paper presents the development of a simulation model of a biomass-fueled boiler coupled to an organic Rankine cycle using scroll expander. The model is validated on experimental data and is used to predict system performances.

## MODELING

### Biomass boiler model

The boiler model is an assembly of an adiabatic combustion chamber and of two (gas-water and water-environment) heat exchangers (ASHRAE Toolkit, 1994).

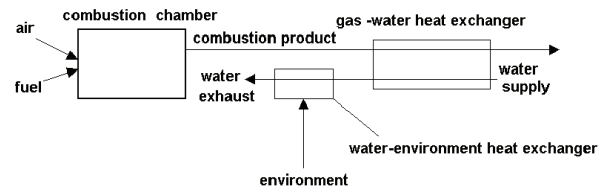


Figure 1 Biomass burner model

The combustion chamber is modelled by a set of four fictitious processes (Figure 2) :

1. Bringing air to the reference temperature of 25°C

$$\dot{Q}_1 = \dot{M}_a \cdot c_{pa} \cdot (T_{ref} - T_{a,su})$$

2. Bringing the fuel to the reference temperature of 25°C  

$$\dot{Q}_2 = \dot{M}_f \cdot c_{p,f} \cdot (T_{ref} - T_{f,su})$$
3. Stoichiometric combustion at 25°C  

$$\dot{Q}_3 = -\dot{M}_f \cdot LHV_f$$
4. Heating-up the combustion products up to the exhaust temperature  

$$\dot{Q}_5 = \dot{M}_g \cdot c_{p,g,5} \cdot (T_{adiab} - T_{ref})$$

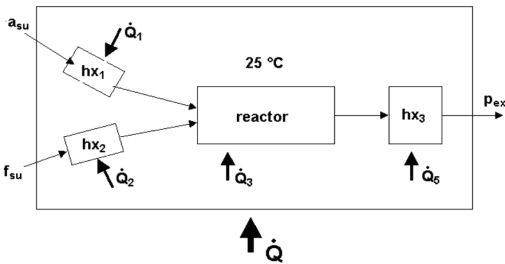


Figure 2 Combustion chamber model

The heat balance over the supposed-to-be combustion chamber gives :

$$\dot{Q}_1 + \dot{Q}_2 + \dot{Q}_3 + \dot{Q}_5 = 0$$

The fuel composition is chosen according to Eskilsson's study on pellet combustion (2003)

### Scroll expander model

The scroll expander model has been previously proposed by Lemort et Al. (2006) and partly validated by tests with steam. In this model, the evolution of the fluid through the expander is decomposed into the following steps (as shown in Fig. 3):

- Supply pressure drop ( $su \rightarrow su,1,1$ )
- Cooling-down in the supply port of the expander ( $su,1,1 \rightarrow su,1$ );
- Isentropic expansion from the supply pressure down to the adapted pressure imposed by the internal expansion volume ratio of the expander ( $su,1 \rightarrow ad$ );
- Expansion at a fixed volume from the adapted pressure to the exhaust pressure ( $ad \rightarrow ex,2$ );
- Mixing between suction flow and leakage flow ( $ex,2 \rightarrow ex,1$ ) and
- Cooling-down or heating-up in the exhaust port ( $ex,1 \rightarrow ex$ ).

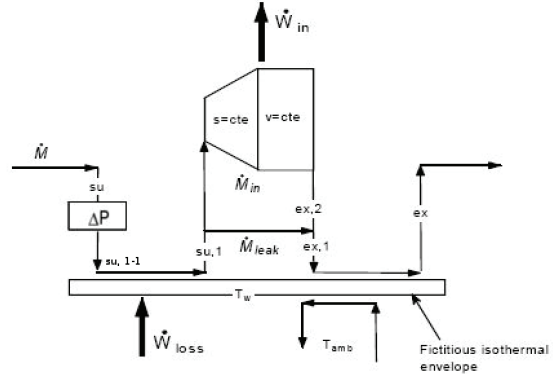


Figure 3 Conceptual scheme of the expander model

The model only requires 9 parameters (heat transfer coefficients, friction torque, leakage area, pressure drop equivalent diameter). Those 9 parameters, defined for a specific type of expander, and for a specific working fluid, need to be determined on the basis of experimental data.

### Condenser and evaporator models

The condenser and the evaporator are modeled by means of the  $\varepsilon$ -NTU method for counter-flow heat exchangers. The heat exchanger is subdivided into 3 zones, each of them being characterized by a heat exchange coefficient AU. Figure 4 shows the 3-zones heat exchanger in the case of an evaporator.

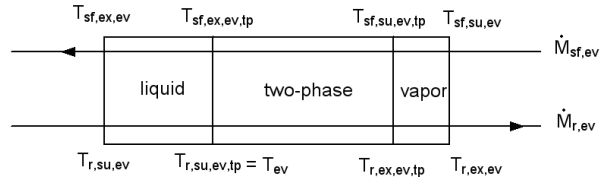


Figure 4 Three zones evaporator

The AU heat transfer coefficient is calculated by considering two resistances in series (secondary fluid and refrigerant sides). These two resistances are calculated as a function of the corresponding mass flow rates ( $C_{sf}$  and  $C_r$  are parameters of the model)

$$AU = \frac{1}{R_{sf} + R_r} = \frac{1}{C_{sf} \dot{M}_{sf}^{0.8} + C_r \dot{M}_r^{0.8}}$$

### Pump model

The pump is modeled by its swept volume, its isentropic efficiency ( $\eta_{pp,s}$ ) and its motor efficiency ( $\eta_{pp,m}$ ). The two latter are supposed to be constant. The fluid heating-up introduced by the pump is neglected. The pump electrical consumption and the fluid flow rate are given by :

$$\dot{W}_{m,pp} = \frac{\dot{W}_{sh,pp}}{\eta_{pp,m}} = \frac{\dot{W}_{pp,s}}{\eta_{pp,s} \cdot \eta_{pp,m}}$$

$$\dot{M}_r = \frac{\dot{V}_{s,pp}}{V_{r,su,pp}} = \frac{X_{pp} \cdot \dot{V}_{s,pp,max}}{V_{r,su,pp}}$$

## EXPERIMENTAL VALIDATION

### Test bench description

An experimental study is carried out on a prototype of ORC working with HCFC-123. The study aims at characterizing the scroll expander, which is originally an oil-free open-drive air scroll compressor, adapted in expander mode. The heat source consists in a set of heat exchangers supplied with hot air. The condenser is cooled by water (Figure 5).

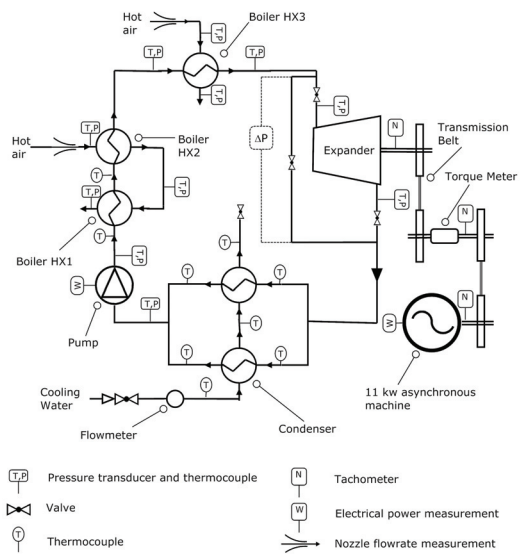


Figure 5 Schematic representation of the test bench

### Reached performances

A series of 39 tests is conducted, by varying pressure ratio (2.7 to 5.4), expander inlet fluid overheating (4 to 71 K), refrigerant flow rate (45 to 86 g/s) and expander rotating speed (1771 to 2660 rpm). A shaft power ranging from 0.38 to 1.82 kW is developed, corresponding to a mechanical isentropic effectiveness ranging from 43 to 68%.

This mechanical isentropic effectiveness is defined by:

$$\varepsilon_s = \frac{\dot{W}_{sh}}{\dot{M}_r \cdot (h_{r,su,exp} - h_{r,ex,exp,s})}$$

### Model validation

The expander model parameters are identified on the basis of test results. The parameters are adjusted to fit the three model outputs (supply pressure, exhaust temperature, shaft power) to experimental data. The *input* variables of this calculation are: expander rotation speed, fluid flow rate, supply temperature and exhaust pressure. An error-objective function is defined, that should be minimized : this error function is a weighted sum of the relative errors for each *output*. It is defined as follows :

$$F = \sum_{i=1}^{39} \left[ \left( \frac{T_{r,ex,exp,meas} - T_{r,ex,exp,pred}}{60} \right)_i^2 + \left( \frac{p_{r,su,exp,meas} - p_{r,su,exp,pred}}{p_{r,su,exp,meas}} \right)_i^2 + \left( \frac{\dot{W}_{sh,exp,meas} - \dot{W}_{sh,exp,pred}}{2 \cdot \dot{W}_{sh,exp,meas}} \right)_i^2 \right]$$

The parameters that minimize the objective function F are identified by means of a genetic algorithm.

Given these parameters, the predicted and measured *outputs* can be compared. This is done in figures 6 to 8.

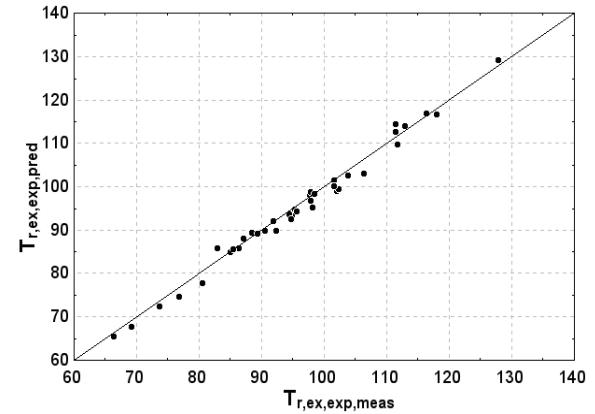


Figure 6 Predicted vs measured expander exhaust temperature

Figure 6 shows the agreement between predicted and measured expander exhaust temperature. A maximum error of 3 K is reached.

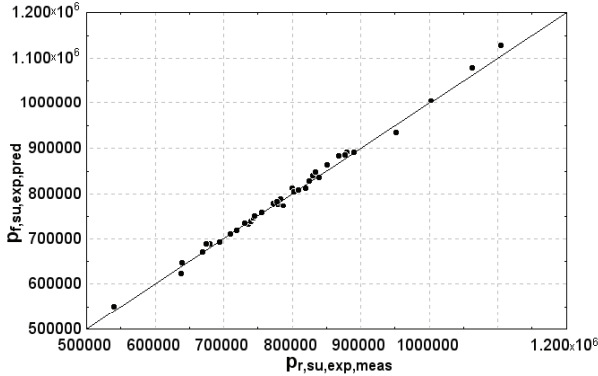


Figure 7 Predicted vs measured expander supply pressure

Figure 7 shows a good prediction of the expander supply pressure, with a maximum relative error of 2.3%. The maximum error in the prediction of the shaft power is 8% (Figure 8).

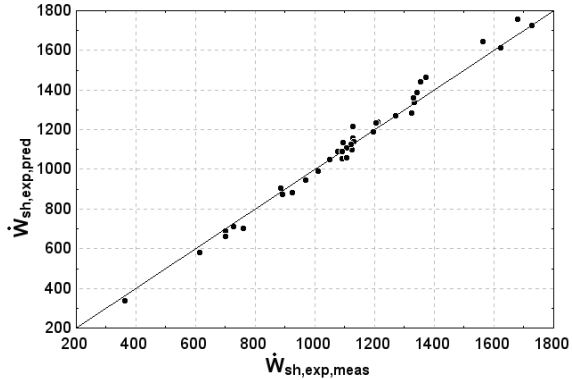


Figure 8 Predicted vs measure expander shaft power

## SYSTEM SIMULATION

This section illustrates how the models developed previously can be used to easily simulate a cogeneration system. Realistic parameters of the scroll expander (which is the least known component) are identified with the experimental data and used in the simulation.

Models of each component are connected together in order to build the whole cogeneration system model (Shown in Figure 9).

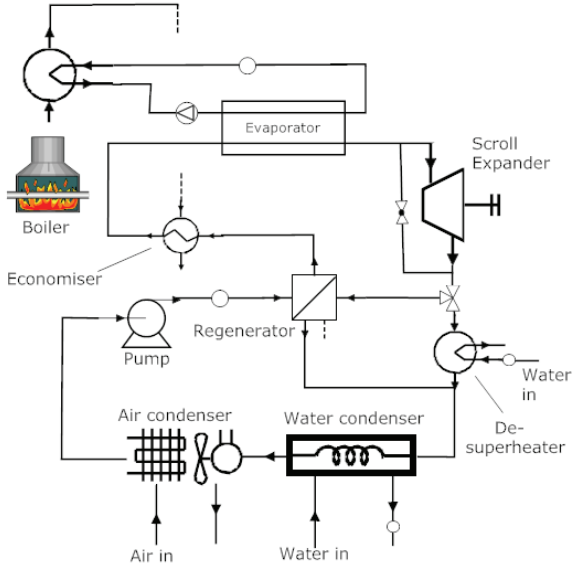


Figure 9 Conceptual scheme of the studied cogeneration system

As shown in Figure 9, heat is transferred from the boiler to the evaporator by means of primary pressurized water circuit. R-123 working fluid, in overheated state at the evaporator exhaust, is expanded in the scroll expander. Two heat exchangers connected in parallel are installed between the expander and the condenser : a regenerator and an additional heat exchanger providing high temperature water. Flow rate repartition between those two exchangers is set by the high temperature water demand.

The low pressure vapor is condensed in two successive heat exchangers : the water condenser is used to provide hot water for space heating and the air condenser is used in case of low space heating demand.

The condensed fluid is pumped successively to the regenerator, the economiser and the evaporator. The economiser is connected to the boiler flue gases in order to preheat the fluid.

This cogeneration system follows a low-temperature, modular approach : the ORC can be plugged to any type of boiler that can produce pressurized hot water in temperature ranging from 100 to 200°C. Since this hot source temperature is quite low, the efficiency of the cycle is lower than in traditional cogeneration systems. However, this lower efficiency is compensated by the simpleness and the lower cost of the system.

For the need of the simulation, and to define a nominal case, the following hypothesis are assumed :

- Boiler inlet/outlet water temperature : 140/150°C
- Pump flow rate adjusted in such a way that overheating at expander supply is 10K.
- Refrigerant charge adjusted in such a way that subcooling at the condenser exhaust is 5K.
- Water temperature at condenser inlet/outlet : 40/60°C
- Heat demand : 600 kW at the water condenser level, no heat demand in the air condenser.
- No high temperature water demand
- Evaporator and condenser exchange area adapted in such a way that their pinch point is 10 K and 5 K respectively.
- Pump effectiveness set to 60 %
- Single-phase heat exchangers effectiveness set to 70%.
- Working fluid : R-123

Two different expander types are defined : The open-drive oil-free air expander defined above, and a hermetic lubricated expander. The parameters of this last expander are evaluated on the basis of the compressor manufacturer data (in compressor mode). Both expanders are described in table 1.

The swept volumes of both expanders are too low for the refrigerant flow rate in this application. Several expanders are hence assembled in parallel. The required number of expanders is calculated by the model.

Type	Compressor swept volume	Volume ratio
Hermetic Lubricated	486.2 cm <sup>3</sup>	3.2
Open-drive Oil-free	148 cm <sup>3</sup>	4.1

Table 1 Expander characteristics

In the case of the open-drive expander, the mechanical shaft power is predicted by the model. An hypothetical electrical generator efficiency of 90% is introduced in the simulation.

#### Definition of the performance indicators :

In cogeneration systems, output electrical power is more valuable than heat output power. Therefore, one single performance indicator is not enough to characterize the system.

Three performance indicators are defined as follows :

$$\text{Net electrical power : } \dot{W}_{el, net} = \dot{W}_{el, exp} - \dot{W}_{el, pp}$$

$$\text{Cycle electrical efficiency: } \eta_{cycle} = \frac{\dot{W}_{el, net}}{\dot{Q}_{ev} + \dot{Q}_{econ}}$$

$$\text{Global efficiency : } \eta_{global} = \frac{\dot{W}_{el, net} + \dot{Q}_{cd}}{\dot{Q}_{tot, boil}}$$

#### Selection of the working fluid

From a first screening of the available working fluids in the temperature range considered, 4 candidates are selected for the simulations : R-245fa, R-123, n-pentane and isopentane. Those fluids are presented in table 2 with their environmental impact and their safety level.

Refrigerant	Atmospheric lifetime [years]	Safety	ODP	GWP	Phase out Year
R-123	1.4	Toxic	0.012	120	2030
R-245fa	7.2	Toxic	-0	950	-
n-pentane	N/A	Flammable	-0	-20	-
isopentane	N/A	Flammable	-0	-20	-

Table 2 Environmental impact of the 4 selected fluids

Source : ASHRAE Refrigeration Handbook (2002)

The main simulation results are presented in table 3.

Refrigerant	$\eta_{cycle}$ [%]	$W_{el, net}$ [kW]	$\eta_{global}$ [%]	$n_{exp}$ [-]	$r_p$ [-]	$P_{ev}$ [bar]	$W_{pp}$ [W]
R-123	8.29	54.93	92.69	5.52	4.52	14.6	5025
R-245fa	7.05	45.86	93.12	3.17	4.51	23.3	11598
R-601 (n-pentane)	8.16	54.37	91.84	7.23	4.59	11.0	4063
R-601a (isopentane)	8.29	55.14	92.03	6.24	4.33	13.1	5054

Table 3 Influence of the working fluid on cycle performances

Table 3 shows that the best electrical efficiency is reached with fluids R-123 and isopentane. However, each fluid shows advantages and drawbacks : isopentane shows a good efficiency, but its specific volume in vapor state is elevated and more expanders in parallel are needed. R-123 also leads to good cycle efficiency, but has a non-null ODP and will be phased out in 2030. R-245fa shows a very high GWP, but few expanders are needed.

For the present application, R-123 is selected as a good compromise between efficiency, safety level and environmental impact.

#### Selection of the expander

The 2 expanders described above are alternatively integrated into the cycle and a simulation is run on the nominal case. The results are described in table 4.

Expander	Expander effectiveness $\varepsilon_s$	cycle efficiency $\eta_{cycle}$
Open drive, oil-free	63.9 %	8.7 %
Hermetic, lubricated	60 %	8.3 %

Table 4 Expander and cycle performances

The hermetic expander shows a slightly lower efficiency, due to a lower built-in volume ratio, and thus increased inadaptation losses. However, this hermetic expander is selected for the present application, since it presents no risk of leakage.

The expander effectiveness shows a maximum when the built-in volume ratio is adapted to the imposed pressure ratio. In the present application, the ideal built-in volume ratio is 4.8, which is superior to the volume ratio of the two expanders described above.

### Influence of the working temperatures

Figure 10 shows the cycle efficiency and the expander effectiveness as a function of the heat source temperature. When this temperature increases, the pressure in the evaporator and the pressure ratio increase. Expander effectiveness shows a maximum for a temperature of 134°C. This temperature corresponds to an expander adapted in terms of volume ratio to the imposed pressure ratio. For temperatures higher than 134°C, the higher the temperature, the higher the under-expansion. This under-expansion explains the maximum in cycle efficiency around 172°C. On the contrary, when the expander internal built-in volume ratio is adapted to the given pressure ratio, no maximum of cycle efficiency is observed.

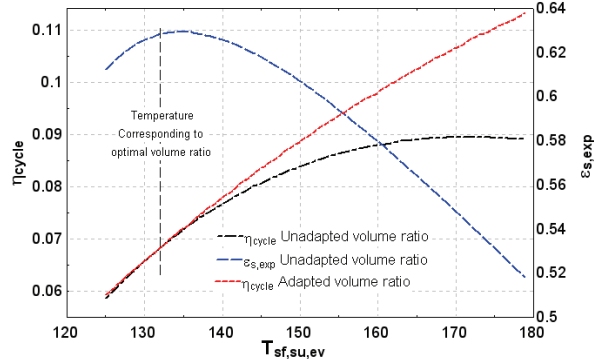


Figure 10 Influence of heat source temperature on expander effectiveness and cycle efficiency

This analysis is performed for heat source temperature, but the same analysis can be applied to heat sink temperature : efficiency will increase if heat sink temperature is decreased, until a maximum is reached.

### Influence of regenerator effectiveness

Figure 11 shows cycle efficiency as a function of regenerator effectiveness for several secondary fluid temperatures in the condenser. This efficiency can be improved by more than 1% when using a regenerator. This improvement is however more limited when the condenser temperature is higher, because of a smaller de-superheating zone.

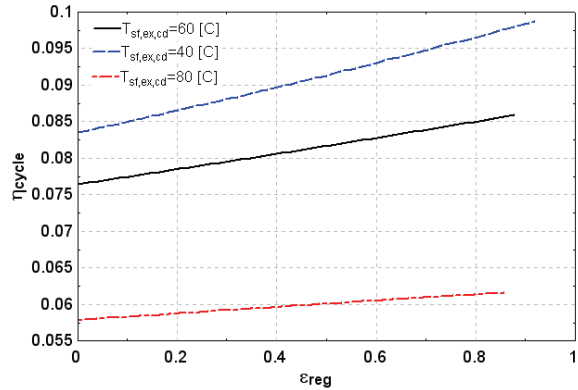


Figure 11 Influence of regenerator effectiveness and heat sink temperature on cycle efficiency

### Influence of economiser effectiveness

Figure 12 shows the evolution of global efficiency and the cycle efficiency with the economiser effectiveness. The economiser lowers the flue gases temperature and consequently improves the global efficiency. Figure 12 also shows that the economizer has no influence on cycle efficiency.

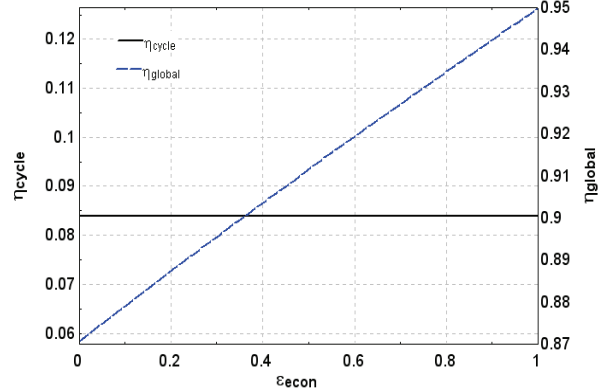


Figure 12 Influence of economiser effectiveness on cycle efficiency and global efficiency

## Influence of high temperature water demand

Figure 13 shows the influence of the high temperature ( $80^{\circ}\text{C}$ ) water demand in the desuperheater heat exchanger. Cycle efficiency and net output power decrease with high temperature water demand, because flow rate in the vapor side of the regenerator is reduced.

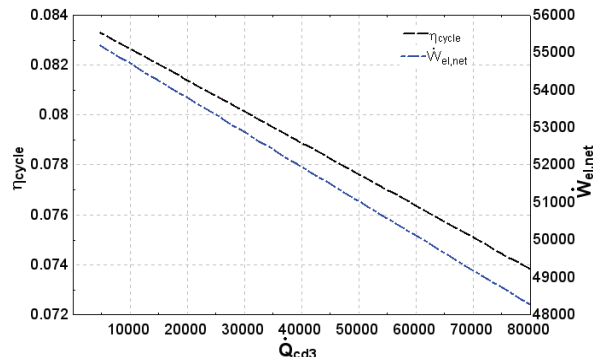


Figure 13 Influence of high temperature water demand on cycle efficiency and net output electrical power

## NOMENCLATURE

AU	heat exchange coefficient	(W/K)
c	Specific heat	(j/kg K)
$\varepsilon$	Effectiveness	(-)
$\eta$	Efficiency	(-)
F	Objective function	(-)
H	Enthalpy	(j/kg)
LHV	Lower Heating Value	(j/kg)
$\dot{M}$	mass flow rate	(kg/s)
N	rotational speed	(Hz)
p	pressure	(Pa)
$\dot{Q}$	heat flux	(W)
R	Thermal resistance	(m <sup>2</sup> K/W)
T	temperature	(°C)
V <sub>s</sub>	swept volume	(m <sup>3</sup> )
v	specific volume	(m <sup>3</sup> /kg)
$\dot{V}$	volume flow rate	(m <sup>3</sup> /s)
$\dot{W}$	power	(W)
X	pump capacity ratio	(-)

## CONCLUSION

The simulation model of a cogeneration system is developed and validated with experimental data.

This model is used to simulate a boiler coupled to an Organic Rankine cycle using scroll expander. An efficiency close to 8% is reached for a heat source and heat sink temperatures of 150 and 60 °C respectively. This efficiency could be increased by increasing heat source temperature, but would require major modification of the boiler design and higher investment costs.

A fluid comparison is performed and shows slightly lower performances for R-245fa in the range of temperatures considered.

The two different scroll expanders (hermetic and open-drive) considered show very similar performances.

The parametric studies highlight the importance of the scroll expander internal built-in volume ratio and show that this ratio should be increased to improve performances. The use of a regenerator and of an economiser conducts to increases of cycle efficiency and of global efficiency of about 1% and 5% respectively.

## Subscripts :

a	air
adiab	adiabatic
amb	ambient
boil	boiler
cd	condenser
econ	economiser
ex	exhaust
exp	expander
f	fuel
l	liquid
leak	leakage
meas	measured
pp	pump
r	refrigerant
ref	reference
reg	regenerator
s	isentropic
sf	secondary fluid
sh	shaft
su	supply
tp	two-phase
v	vapor
w	water

## REFERENCES

- Bourdouxhe, J-P., Grodent, M., Lebrun, J., Saavedra C., ‘A Toolkit for Primary HVAC System Energy Calculation – Part 1 : Boiler Model’, *ASHRAE Transactions*, vol. 100, Part 2, ASHRAE, 1994
- R. G. Doerr, K. Lilje, ‘Refrigerant system chemistry’, *ASHRAE Refrigeration Handbook*, Chapter 5.3, 2002
- D. Eskilsson, M. Ronnback, J. Samuelsson, C. Tullin, ‘Optimisation of efficiency and emissions in pellet burners’, *Biomass and Bioenergy* 27, pp. 541–546, 2004
- Kane, El H. 2002. ‘Intégration et optimisation thermoéconomique & environnementale de centrales thermiques solaires hybrides’. *PhD Thesis*, Laboratoire d’Energétique Industrielle, Ecole polytechnique Fédérale de Lausanne, Suisse.
- V. Lemort, I.V. Teodorese, J. Lebrun, ‘Experimental Study of the Integration of a Scroll Expander into a Heat Recovery Rankine Cycle’, *The 18th International Compressor Engineering Conference*, Purdue, USA, July 17-20, 2006
- Manzagol, J., P. d’Harbouillé, G. Claudet, and G. Gistau Baguer. 2002. ‘Cryogenic scroll expander for Claude cycle with cooling power of 10 to 100 watts at 4.2 K’. *Advances in Cryogenic Engineering*, CEC AIP Conference Proceedings 613: 267-274.
- P. Platell, ‘Displacement expanders for small scale cogeneration’, Licentiate thesis, Royal Institute of Technology, Stockholm, 199
- Xiaojun, G., L. Liansheng, Z. Yuanyang, S. Pengcheng. 2004. ‘Research on a Scroll Expander Used for Recovering Work in a Fuel Cell’. *International Journal of Thermodynamics* 7:1-8.
- Zanelli R., D. Favrat. 1994. ‘Experimental Investigation of a Hermetic Scroll Expander-Generator’, *Proceedings of the 12<sup>th</sup> International Compressor Engineering Conference at Purdue*: 459-464.
- Yuanyang, Z., L. Liansheng, and S. Pengcheng. ‘Thermodynamic simulation of scroll compressor/expander module in automotive fuel cell engine’, Proc. IMechE 220 Part D: *J. Automobile Engineering*, 2006.